EJCRIM
European Journal
of Case Reports
in Internal Medicine

CHECK THE CALCIUM FIRST IN ANY BONE LESION: BROWN TUMOUR OF THE TALUS MISINTERPRETED AS GIANT CELL TUMOUR

Özlem Eren[1], Ümit Çavdar[1], Ali Salbas[2], Aslı Irmak Akdoğan[2], Kadir Alper Küçüker[3], Aslı Kahraman[4], Barış Önder Pamuk[1]

[1] Department of Endocrinology and Metabolism, Atatürk Training and Research Hospital, Kâtip Çelebi University, İzmir, Turkey
[2] Department of Radiology, Atatürk Training and Research Hospital, Kâtip Çelebi University, İzmir, Turkey
[3] Department of Nuclear Medicine, Atatürk Training and Research Hospital, Kâtip Çelebi University, İzmir, Turkey
[4] Department of Pathology, Atatürk Training and Research Hospital, Kâtip Çelebi University, İzmir, Turkey

Corresponding author's e-mail: ozlemeren138@gmail.com

Received: 22/09/2025
Accepted: 13/10/2025
Published: 22/10/2025

Conflicts of Interests: The Authors declare that there are no competing interests.
Patient Consent: Written informed consent was obtained from the patient for the publication of this article.
This article is licensed under a Commons Attribution Non-Commercial 4.0 License

How to cite this article: Eren O, Çavdar U, Salbas A, Akdoğan AI, Küçüker KA, Kahraman A, Pamuk BO. Check the calcium first in any bone lesion: brown tumour of the talus misinterpreted as giant cell tumour. *EJCRIM* 2025;**12**:doi:10.12890/2025_005862

ABSTRACT

Introduction: Although the vast majority of bone tumours are benign, they are a heterogeneous group of lesions with a wide spectrum of biological properties. Osteolytic, osteoblastic, or mixed-pattern changes may be observed, reflecting the heterogeneity of the underlying pathophysiological processes. Osteolytic lesions, most commonly arising from metastatic disease, multiple myeloma, or hyperparathyroidism, are the most frequently encountered presentations in clinical practice.
Case presentation: Here, we report the case of a 59-year-old woman with a 3-month history of right ankle pain, in whom radiological evaluation revealed an osteolytic talar lesion initially interpreted as a giant cell tumour (GCT) and surgically excised. During postoperative oncological evaluation, a parathyroid adenoma was detected, and the patient was referred to our endocrinology clinic. Laboratory results were consistent with primary hyperparathyroidism. Re-evaluation of the bone pathology, in light of the biochemical and radiological findings and the absence of H3F3A immunostaining, supported the diagnosis of a brown tumour (BT). Following parathyroidectomy, laboratory results normalized.
Discussion: Since hypercalcemia is not typically observed in GCTs, its presence should raise suspicion for metastatic or granulomatous diseases, as well as BTs associated with hyperparathyroidism. Upon detection of hypercalcemia, parathyroid hormone (PTH) levels should be evaluated as part of the differential diagnosis. Subsequent histopathological and immunohistochemical analyses can help distinguish these entities, with H3F3A immunostaining serving as an important marker for differentiating GCTs from BTs.
Conclusion: This case highlights the importance of assessing serum calcium and parathyroid hormone levels, together with relevant clinical, radiological, and histopathological findings, to establish an accurate diagnosis in patients presenting with bone lesions.

KEYWORDS

Hyperparathyroidism, giant cell tumour of bone, osteitis fibrosa cystica, hypercalcemia

EFIM
European Federation of Internal Medicine

Publisher
smc media srl

LEARNING POINTS

- Serum calcium and parathyroid hormone measurements are essential in the evaluation of bone lesions. Hypercalcemia may indicate primary hyperparathyroidism but can also occur in myeloma, metastases, or granulomatous diseases.
- Brown tumours (BTs) and giant cell tumours (GCTs) of bone may overlap; BTs are associated with hypercalcemia and H3F3A negativity, while GCTs are characterized by normal calcium levels and H3F3A positivity.
- A multidisciplinary approach combining clinical, biochemical, and pathological data improves diagnostic accuracy in bone lesions by distinguishing benign, malignant and metabolic causes, ensuring appropriate management.

INTRODUCTION

While the majority of bone tumours are benign, malignant forms account for approximately 10% of cases[1]. Key considerations in the evaluation of bone tumours include patient age, tumour location, and radiological features.

Radiologically, bone tumours are classified as osteolytic, osteoblastic, or mixed, depending on the predominant pattern of bone change. Osteolytic lesions are frequently seen in clinical practice and are most often caused by metastases, multiple myeloma, or primary bone tumours such as giant cell tumour (GCT). Granulomatous diseases, including Langerhans cell histiocytosis and sarcoidosis, as well as brown tumours (BTs) associated with hyperparathyroidism, may share similar radiological findings.

Bone lesions associated with hypercalcemia are most commonly observed in osteolytic metastases, multiple myeloma, granulomatous diseases, and BTs, where increased osteoclastic activity or enhanced vitamin D metabolism leads to hypercalcemia with variable phosphate levels. Therefore, measurement of both serum calcium and parathyroid hormone (PTH) levels is essential for differentiating among these bone lesions.

Here, we report a case of a solitary osteolytic lesion of the talus presenting with bone pain, initially diagnosed as a GCT. During follow-up, a parathyroid adenoma was incidentally discovered, leading to endocrinological evaluation. This report discusses the diagnostic pathway and highlights key considerations in the differential

CASE DESCRIPTION

A 59-year-old woman with no known comorbidities presented to a primary care clinic with a 3-month history of

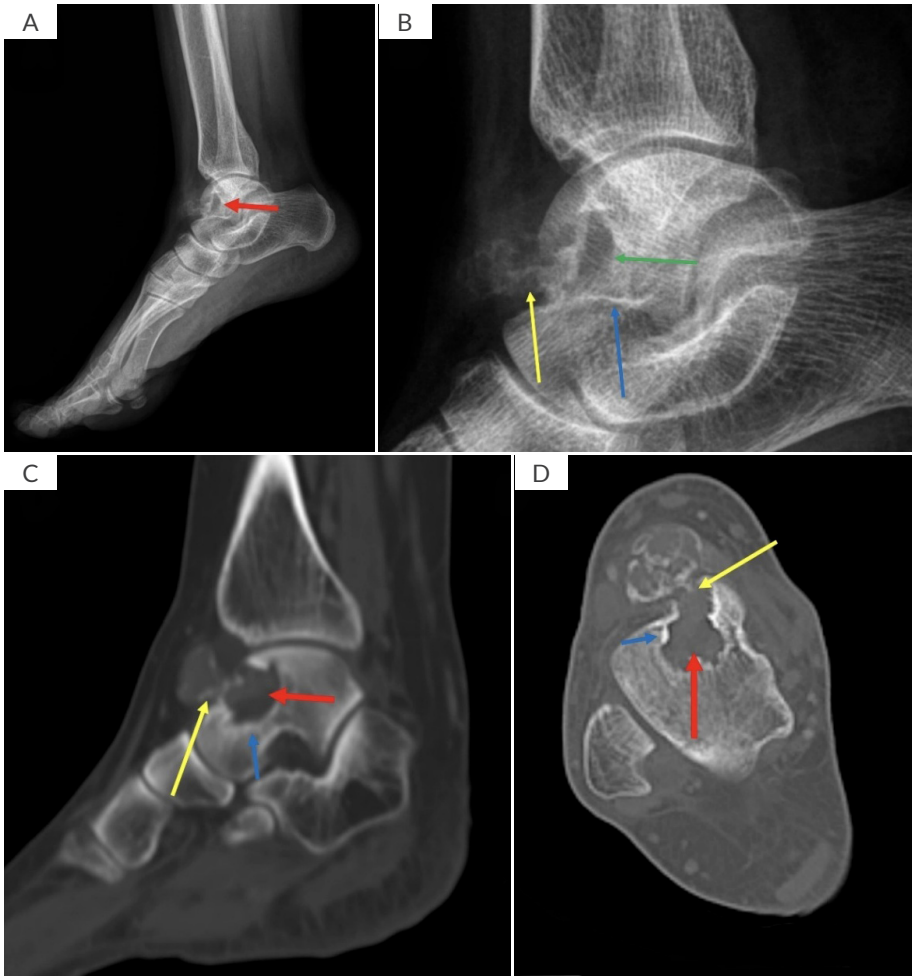


Figure 1. Conventional radiographs of the ankle. A) Lateral view showing an expansile lytic lesion in the talar body (red arrow). B) Magnified view demonstrating its expansile nature (green arrow), cortical defect (yellow arrow), and peripheral sclerotic–calcific changes (blue arrow). Non-contrast computed tomography images of the ankle. C) Sagittal section showing expansile lytic lesion (red arrow) with anterior cortical breach (yellow arrow) and peripheral calcifications (blue arrow). D) Axial section confirming cortical destruction and peripheral calcifications.

right ankle pain. Lateral radiography showed an expansile lytic lesion in the talus with cortical thinning, disruption, and peripheral sclerosis *(Fig. 1)*. The patient was referred to a tertiary orthopaedic department for further evaluation. A computed tomography (CT) scan of the right ankle showed a cortical defect with dorsal extension and peripheral sclerotic and calcific changes *(Fig. 1)*.

Magnetic resonance imaging (MRI) demonstrated a predominantly hypointense lesion on T1-weighted images, with cystic components, fluid–fluid levels, and posterior contrast enhancement *(Fig. 2)*.

Based on the overall radiological appearance, a GCT of bone with an associated aneurysmal bone cyst component was considered. A talar biopsy was initially consistent with GCT and aneurysmal bone cyst, and surgical excision was performed by the orthopaedics team. Histopathology showed fibroblastic stroma with hemosiderin pigment and multinucleated giant cells, findings consistent with GCT.

The patient was referred to oncology, where a postoperative CT scan incidentally revealed a parathyroid adenoma and thyroid nodule without evidence of metastatic disease. The patient was subsequently referred to endocrinology for further management.

Laboratory evaluation demonstrated calcium 13.7 mg/dl (N: 8.5–10.5), phosphorus 2.8 mg/dl (N: 2.5–4.5), parathyroid hormone (PTH) 869 ng/l (N: 18.5–88), vitamin D 8 µg/l (N: 30–70), alkaline phosphatase (ALP) 250 U/l (N: 30–120), erythrocyte sedimentation rate (ESR) 13 mm/h (N:0-30), haemoglobin 13.8 g/dl (N:11-15), albumin 45 g/l (N: 35–52), and globulin 25 g/l (N: 20–35). These laboratory findings were primarily consistent with primary hyperparathyroidism (PHPT) and were not suggestive of malignant aetiology. The patient was then admitted to our endocrinology clinic for further evaluation. Intravenous hydration and oral vitamin D replacement were initiated. Dual-energy X-ray absorptiometry (DXA) revealed a T-score of 3.9 at the lumbar spine (L1–L4) and 1.5 at the femoral neck. Following a 5 mg intravenous zoledronic acid infusion, the serum calcium decreased to 10.5 mg/dl. Neck ultrasound revealed a 35 × 13 mm hypervascular lesion posterior to the right thyroid lobe and a 4 mm irregularly marginated nodule within the right thyroid lobe. Parathyroid scintigraphy confirmed intense technetium 99m sestamibi (Tc-99m MIBI) uptake in the lesion, further supporting the diagnosis of parathyroid adenoma *(Fig. 3)*.

Given the biochemical and imaging findings consistent with PHPT associated with parathyroid adenoma, along with the uncommon location of the lesion for a GCT, the patient was re-evaluated, and the histopathological specimens were re-examined. In addition to the presence of fibroblastic stroma, hemosiderin pigment, and multinucleated giant cells, immunohistochemical staining for H3F3A was negative, supporting a revised diagnosis of a BT associated with PHPT *(Fig. 4)*.

Review of a cranial CT scan performed 3 years earlier revealed a "salt-and-pepper" skull, consistent with hyperparathyroidism. Current skull radiography showed similar findings *(Fig 5)*. No other skeletal lesions were detected.

The patient underwent right inferior parathyroidectomy and right lobectomy. Histopathology confirmed a 3.5 cm hypercellular parathyroid adenoma and papillary thyroid

	Reference range	Preoperative	Postoperative	One year follow-up
Calcium (mg/dl)	8.5–10.5	13.7	9.6	9.5
Phosphorus(mg/dl)	2.5-4.5	2.8	2.7	2.5
PTH (ng/l)	18.5-88	869	104	76
25-OH-D (µg/l)	20-70	8	20	17.7
Creatinine (mg/dl)	0.6-1.1	0.62	0.6	0.7
ALP (U/l)	30-120	250	108	51
Haemoglobin (g/dl)	11-15	13.8	13	13.5
Albumin (g/l)	35-52	45	42	43
Globulin (g/l)	20-35	25	-	25
ESR (mm/h)	0-30	13	-	18
Femur neck T score	>-1	-1.5	-	-0.8
Lumbar T score	>-1	-3.9	-	-3

Abbreviations: DXA, dual-energy X-ray absorptiometry; PTH, parathyroid hormone; ESR, erythrocyte sedimentation rate; ALP, alkaline phosphatase.

Table 1. The patient's preoperative, postoperative and 1-year follow-up laboratory and DXA results.

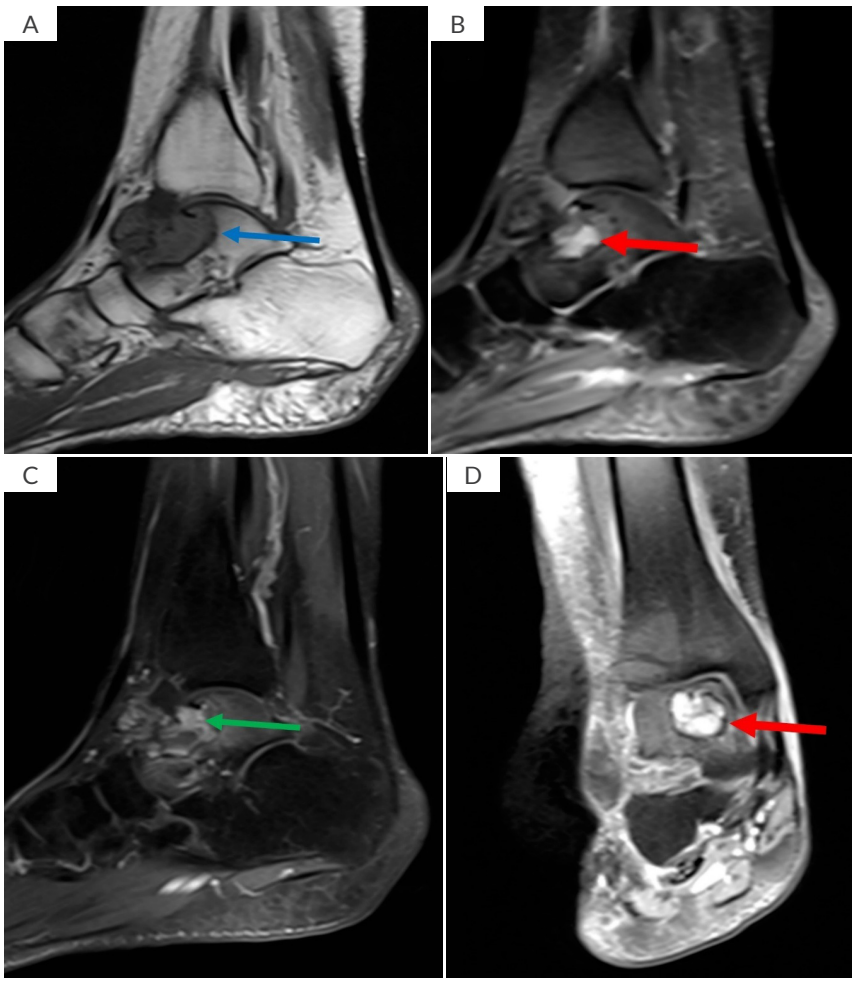


Figure 2. Magnetic resonance imaging of the ankle. A) Sagittal T1-weighted image without fat suppression shows a hypointense lesion centered in the talar body (blue arrow). B) Sagittal fat-suppressed proton density image demonstrates hyperintense cystic components in the posterior portion (red arrow). C) Sagittal post-contrast fat-suppressed T1-weighted image reveals a solid enhancing component posteriorly (green arrow). D) Coronal fat-suppressed proton density image shows fluid–fluid levels within the lesion (red arrow), consistent with aneurysmal bone cyst–like areas. All sequences demonstrate an anterior cortical defect with dorsal extension, correlating with computed tomography and radiographic findings.

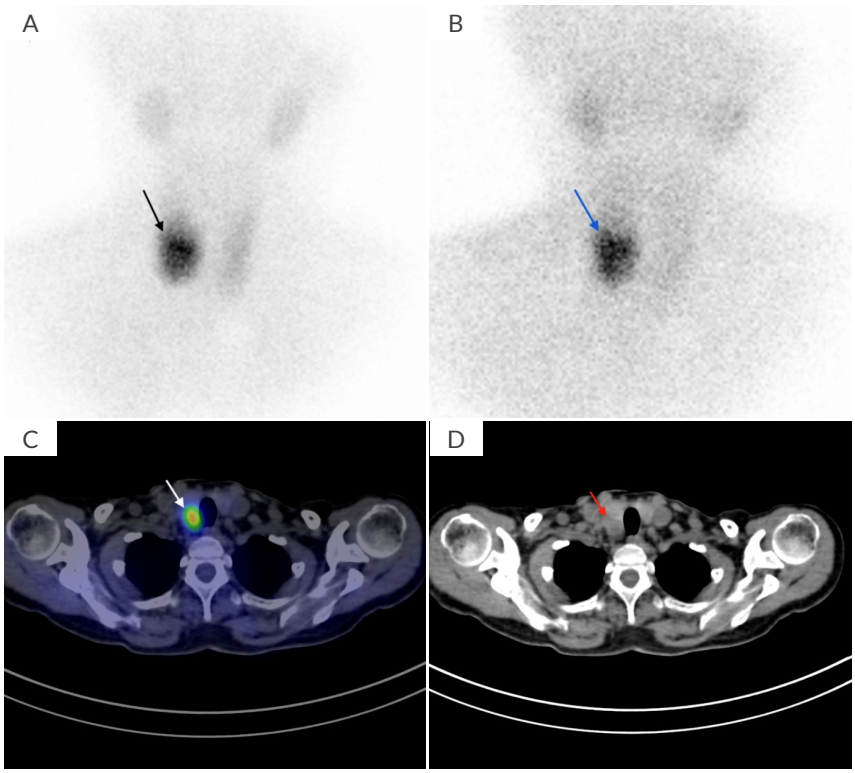


Figure 3. Parathyroid scintigraphy with single photon emission computed tomography (SPECT)/computed tomography (CT) correlation. A) Early-phase static image showing nodular increased uptake in the region of the right lower thyroid lobe (black arrow) with diffuse mild uptake in the remainder of the gland. B) Late-phase image demonstrating persistent nodular uptake in the right lobe (blue arrow) and washout of background thyroid activity. C, D) SPECT/CT images acquired after late static imaging reveal a nodule with intense radiopharmaceutical uptake posterior to the right thyroid lobe (C, white arrow; D, red arrow), consistent with parathyroid adenoma.

microcarcinoma. Postoperatively, calcium and phosphorus levels normalized, and vitamin D therapy was continued. At 1 year, the patient remained asymptomatic with normal calcium, phosphorus, and PTH levels. Preoperative, postoperative, and one-year follow-up laboratory and DXA results are summarized in *Table 1*.

Bone scintigraphy showed uptake only at the right ankle, corresponding to the site of BT excision, with no additional

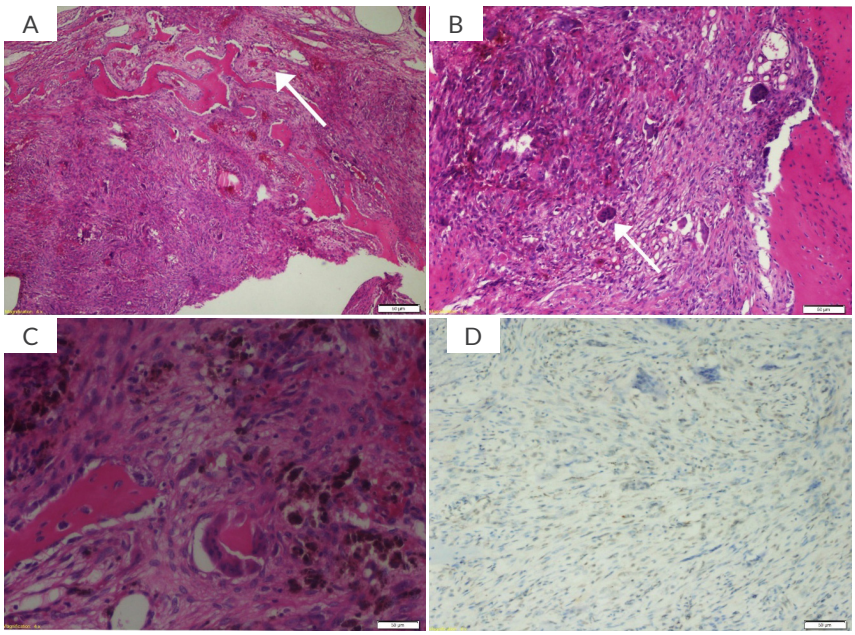


Figure 4. Histopathological examination of the talar lesion. A) Fibroblastic stroma with hemosiderin deposits and scattered multinucleated giant cells near bone trabeculae (arrow), consistent with a brown tumour. B) Osteoclast-type giant cells (arrow) within fibrous stroma, with irregular distribution, haemorrhage, and hemosiderin deposition supporting a reparative/ reactive process. C) Higher magnification showing hemosiderin-laden macrophages, multinucleated giant cells, and bony trabeculae within a fibroblastic background. D) H3F3A immunohistochemistry is negative, excluding H3F3A-mutant giant cell tumour of bone.

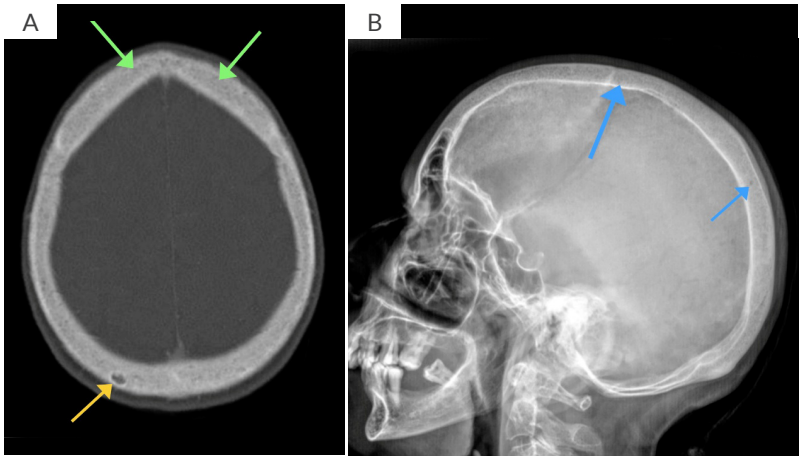


Figure 5. A) Axial non-contrast cranial computed tomography (CT) scan of the patient from 3 years earlier: a bone window image demonstrates expansion of the diploic space and multiple small lytic foci throughout the calvarial bones (green arrows), consistent with the characteristic "salt and pepper" appearance of hyperparathyroidism. A tiny lytic lesion is also observed in the posterior aspect of the right parietal bone (yellow arrow). B) Lateral skull radiograph shows similar findings, including widened diploic space and numerous punctate lucencies (blue arrows), again suggestive of the salt and pepper pattern.

lesions. The patient received 5 mg of zoledronic acid and has remained stable on routine follow-up.

DISCUSSION

BTs are benign osteolytic lesions caused by hyperparathyroidism. Radiologically, BTs and GCTs can appear similar, presenting as lytic, expansile lesions with cortical thinning and peripheral sclerosis. Due to their similarity on imaging, BTs are frequently misdiagnosed as GCTs[2,3].

BTs usually affect females in their third to fifth decades, while GCTs present between 20 and 50 years of age, with peak incidence in the third decade. BTs most commonly occur in the mandible, ribs, pelvis, and clavicle, whereas GCTs typically arise in the distal femur and proximal tibia. Our patient's presentation was unusual both in terms of age and talar involvement. The talus is rarely affected by either entity; in a 25-year case series, the incidence of talar GCT was reported to be only 0.4%[4]. Although talar BTs have been reported in the literature, they are exceedingly rare[5], and this uncommon localization further complicated the diagnostic process.

Another distinctive feature of our case was the solitary nature of the lesion. BTs usually show multifocal skeletal involvement in 2–5% of PHPT cases[6]. In contrast, our patient had a single talar lesion, with only diffuse skeletal changes such as the "salt-and-pepper" appearance of the skull. Because these lesions may not present typically in clinical practice, additional biochemical evaluation is important in the diagnostic process.

When a bone lesion is encountered, serum calcium measurement is a critical first step. Hypercalcemia narrows the differential diagnosis to metastatic disease, multiple myeloma or plasmacytoma, granulomatous disorders (such as sarcoidosis and Langerhans cell histiocytosis), and BTs associated with hyperparathyroidism. In GCT of bone, however, hypercalcemia is not expected. PTH measurement further refines the distinction: elevated PTH in the setting of hypercalcemia with low-to-normal phosphorus supports hyperparathyroidism-related BTs, whereas suppressed PTH with hyperphosphatemia suggests granulomatous disease or malignancy. Similar cases have been reported in which hypercalcemia with osteolytic lesions initially mimicked myeloma or metastasis, but elevated PTH confirmed BTs[7,8]. Histopathology and immunohistochemistry should be performed only after assessing calcium and PTH levels. At

the pathological stage, it is crucial to inform the pathologist about serum calcium and PTH levels, as lesions occurring with or without hypercalcemia often have distinct aetiologies. Additionally, BTs and GCTs may share similar histological features, both containing fibrous stroma, hemosiderin deposits, and multinucleated giant cells. When morphology is equivocal, immunohistochemistry is particularly helpful. In our case, the absence of H3F3A staining in giant cells supported BT, since GCTs typically demonstrate H3F3A positivity[9]. Even in cases of PHPT, GCT of bone may rarely occur[10], and in such cases, H3F3A immunostaining can play an important role in establishing the diagnosis.

In our patient, the lesion was initially considered a GCT; however, subsequent biochemical assessment indicating PHPT, along with histopathological correlation and H3F3A negativity on immunohistochemistry, supported the diagnosis of a BT.

CONCLUSION

This case underscores the importance of integrating radiological, biochemical, and pathological data in the evaluation of bone lesions. Measurement of serum calcium and PTH remains an essential first step, as hypercalcemia should prompt consideration of BT along with malignant and granulomatous causes.

REFERENCES

1. Anderson WJ, Doyle LA. Updates from the 2020 World Health Organization Classification of Soft Tissue and Bone Tumours. *Histopathology* 2021;**78**:644-657. doi: 10.1111/his.14265
2. Hamidi S, Mottard S, Berthiaume MJ, Doyon J, Bégin MJ, Bondaz L. Brown tumor of the iliac crest initially misdiagnosed as a giant cell tumor of the bone. *Endocrinol Diabetes Metab Case Rep* 2020;**2020**:20-0029. doi: 10.1530/EDM-20-0029
3. Hussain A, Shahid F, Ul Ain N. Primary Hyperparathyroidism With Brown Tumor of the Mandible Misdiagnosed as a Giant Cell Tumor: A Case Report. *Cureus* 2024;**16**:e56153. doi: 10.7759/cureus.56153
4. Minhas MS, Khan KM, Muzzammil M. Giant cell tumour of foot bones - 25 years experience in a tertiary care hospital. *J Pak Med Assoc* 2015;**65**:S67-71.
5. Erken HY, Ofluoğlu Ö, Burç H. Unusual Presentation of Brown Tumor in Lateral Malleolus And Talus, A Case Report. *J Clin Anal Med* 2013;**4**: 324-326. doi: 10.4328/JCAM.2326
6. Xu W, Qu Y, Shi W, Ma B, Jiang H, Wang Y, et al. Multiple bone brown tumor secondary to primary hyperparathyroidism: a case report and literature review. *Gland Surg* 2019;**8**:810-816. doi: 10.21037/gs.2019.11.14
7. Duyck J, Spincemaille K, Verfaillie J, Meert C, Muylle K. Widespread presentation of brown tumors mimicking multiple myeloma. *Eur J Hybrid Imaging* 2023;**7**:10. doi: 10.1186/s41824-023-00168-3
8. Parikh P, Shetty S, Rodrigues G, Bhat SN. Brown Tumour Mimicking Skeletal Metastasis. *BMJ Case Reports* 2021;**14**:e243478. doi: 10.1136/bcr-2021-243478
9. Lüke J, von Baer A, Schreiber J, Lübbehüsen C, Breining T, Mellert K, et al. H3F3A mutation in giant cell tumour of the bone is detected by immunohistochemistry using a monoclonal antibody against the G34W mutated site of the histone H3.3 variant. *Histopathology* 2017;**71**:125-133. doi: 10.1111/his.13190
10. Rossi B, Ferraresi V, Appetecchia ML, Novello M, Zoccali C. Giant Cell Tumor of Bone in a Patient with Primary Hyperparathyroidism: A Challenge in Differential Diagnosis with Brown Tumor. *Skeletal Radiology* 2014;**43**:693–697. doi: 10.1007/s00256-013-1770-9